International Journal of Multidisciplinary Research and Development
www.allsubjectjournal.com
ISSN Online: 2349-4182 ISSN Print: 2349-5979
Received: 27-10-2025, Accepted: 26-11-2025, Published: 11-12-2025
Volume 12, Issue 12, 2025, Page No. 104-107

Analysis of the effect of exposure factors and Zn filter thickness on radiographic images in head X-ray examinations

Lutfi Azizah, Pandji Triadyaksa*, Zaenul Muhlisin
Department of Physics, Faculty of Science and Mathematics, Diponegoro University, Indonesia

Abstract

One of the key determinants of image quantity and quality is exposure. Research on the impact of exposure factors and zinc (Zn) filter thickness typically uses quantitative evaluation parameters, such as SNR and CNR. Several studies on the effects of exposure factors and Zn filter thickness using an anthropomorphic head phantom still have limitations, such as a lack of information on how exposure factors and Zn filter thickness affect radiographic images in head examinations. Therefore, this study aims to analyze the influence of variations in exposure factors and Zn filter thickness on SNR and CNR as evaluation parameters in radiographic images. The study used radiographic images of an anthropomorphic head phantom with tube voltage (kV) ranging from 60 kV to 80 kV in 5 kV intervals, tube current-time variations of 50 mAs, 40 mAs, 32 mAs, 25 mAs, and 20 mAs, and Zn filters with thicknesses of 0 mm, 0.2 mm, 0.4 mm, 0.6 mm, and 0.8 mm. The radiographic images of the anthropomorphic head phantom in the soft-tissue area had five ROI sizes with a 5 mm diameter. In the background-intensity area, there were five ROI sizes with a 10 mm diameter. This study analyzed the mean pixel intensity and background intensity, and calculated SNR and CNR values in the images using the Micro Dicom Viewer software. The study found that for soft tissue, the highest SNR was obtained with a 0.4 mm Zn filter (383.54), whereas for hard tissue, the highest SNR was obtained without a Zn filter (2418.66). The highest CNR was also observed without the Zn filter, at 2113.97. The mean and background pixel intensities affect the quantity and quality of radiographic images in head phantom examinations. As the mean and background pixel intensities increase, image quality decreases, as indicated by reductions in SNR and CNR.

Keywords: Exposure Factors, Zn Filter, SNR, CNR

Introduction

Exposure factors play a crucial role in determining the quality and quantity of radiographic images produced during X-ray examinations. These factors include the voltage (kVp), current (mA), and exposure time (s). The voltage influences image contrast, with higher kVp values generally reducing contrast, while current determines the amount of X-rays produced, directly impacting radiation quantity. Exposure time should be kept as short as possible to minimize patient dose and reduce image blurring from patient movement (Bushong, 2001) [3].

Alongside exposure factors, filters are essential for modifying the X-ray beam by removing low-energy radiation, thereby minimizing patient exposure and enhancing image quality. Filters can be classified into inherent, added, and total filtration, all of which affect image density by altering the X-ray beam's energy levels (Fosbinder & Orth, 2002) [7].

Several studies have explored the impact of exposure factors and filter variations on radiographic image quality. Fahmi *et al*. (2008) [5] found that changes in exposure factors during abdominal radiography with computed radiography did not significantly affect image density or contrast, although they reduced patient radiation dose. Trirahayu (2013) [15] examined the effect of copper filter thickness on radiographic contrast and concluded that thicker filters reduced image density. Pardede & Setiawati (2014) [12] investigated the use of different filters and found that aluminum (Al) filters, when combined with stainless steel (SS) and zinc (Zn), produced lower radiation doses and higher image contrast. Similarly, Litasova *et al*. (2018) [10] showed that filter thickness and material composition, such as the combination of Al and Zn, impacted the Entrance Surface Dose (ESE) during head examinations, with thicker filters reducing ESE.

Sparzinanda *et al*. (2018) [14] and Khasanah (2018) [8] focused on the effects of increased exposure time, current, and voltage on image quality and scatter radiation. These studies revealed that higher current and voltage lead to reduced image quality, with the increased voltage contributing to greater pixel count and lower scatter radiation doses. Additionally, zinc filters, due to their higher density compared to aluminum, were found to offer better X-ray absorption and image quality in some studies (Litasova *et al*., 2018) [10].

Previous studies indicate that optimal radiographic image quality is achieved by balancing high voltage, low current, and short exposure times, while also utilizing appropriate filters to minimize radiation exposure. Based on this, the current study aims to explore the relationship between variations in exposure factors and zinc (Zn) filter thickness, with a focus on Signal-to-Noise Ratio (SNR) and Contrast-to-Noise Ratio (CNR) in general head radiography.

Materials and Methods

Exposure parameters

This study was conducted using a General Electric (GE) general radiography unit with a maximum X-ray tube voltage of 150 kVp and an inherent filtration of 1.3 mm Al. The object used was an anthropomorphic head phantom. The tube voltage for anteroposterior (AP) head examinations was varied from 60 to 80 kV in 5 kV increments. An additional filter made of zinc (Zn) was employed with thickness variations of 0, 0.2, 0.4, 0.6, and 0.8 mm. The tube current–time product (mAs) was determined using Equation 1, based on the routine exposure factors for lateral head examinations: a tube voltage of 70 kV, a current–time product of 32 mAs, and a focus–film distance (FFD) of 100 cm.

$$I_2 = 32 \times \left(\frac{70}{kVp_2}\right)^4 \qquad (1)$$

where I_2 is the time-current at the setting voltage (kVp_2). Since the X-ray unit console has specific current–time settings, the mAs variations obtained from Equation 1 must be adjusted to the available mAs options on the console, namely those listed in the fourth column of Table 1.

Table 1. Exposure factors for anteroposterior (AP) cranium examination

No.	Voltage (kV)	Current × Time (According to Eq. 1) (mAs)	Current × Time (Machine option) (mAs)
1	60	59,3	50
2	65	43	40
3	70	32	32
4	75	24,3	25
5	80	18,8	20

Image processing

After the head phantom images were obtained, the mean value and noise were measured using Micro Dicom Viewer. In this application, the imported images are 512 × 512 pixels. An image width of 512 pixels corresponds to a physical length of 36.12 cm; from this information, 1 cm equals 14.1750 pixels, and 1 pixel equals 0.0706 cm. The representation of one square pixel has a value of 0.0050 m³. Figure 1 shows an example of a skull phantom with higher signal intensity than the surrounding soft tissue.

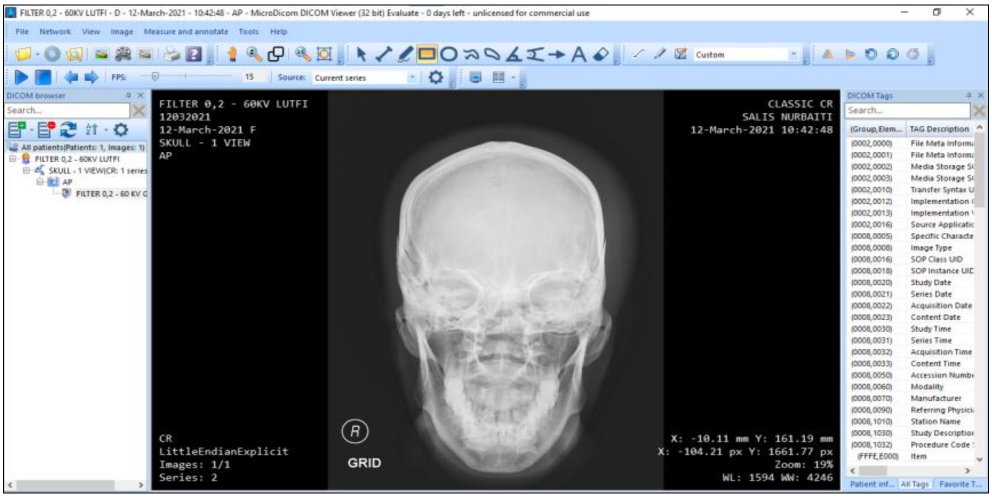

Fig 1: Head phantom representation on the Micro Dicom viewer

The next step was to create Regions of Interest (ROIs) with adjusted sizes. In the head phantom image, three ROI sizes were used: the first ROI, measuring 50 × 50 mm, was placed in the rugged tissue region of the forehead; the second ROI, measuring 5 × 5 mm, was placed in the soft tissue layer (skin) (Figure 2); and the third ROI, measuring 10 × 10 mm, was placed at five different locations in the background of the image (Figure 3). The ROI location selections were conducted to obtain mean pixel intensities representing the soft-tissue distribution and background standard deviations in the head phantom image.

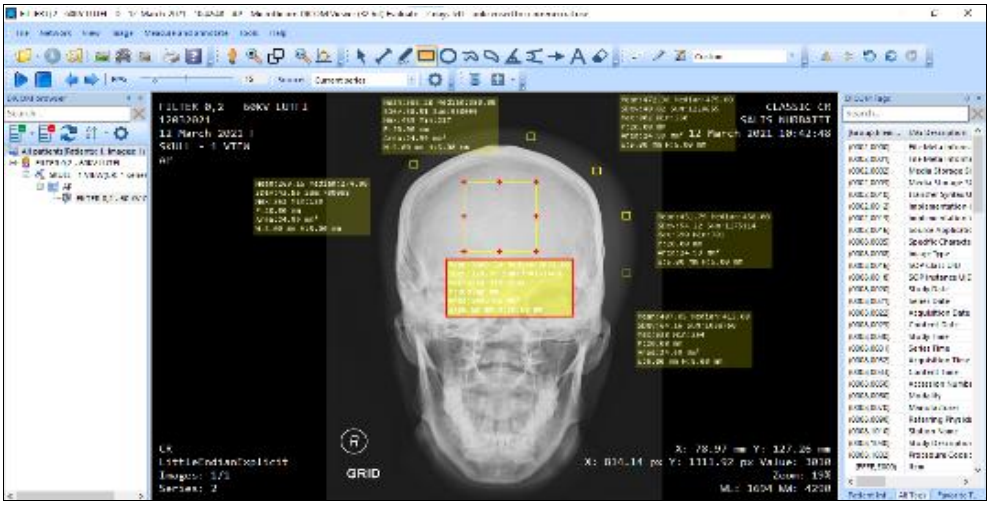

Fig 2: The ROI locations on the forehead and the soft-tissue layer of the head phantom

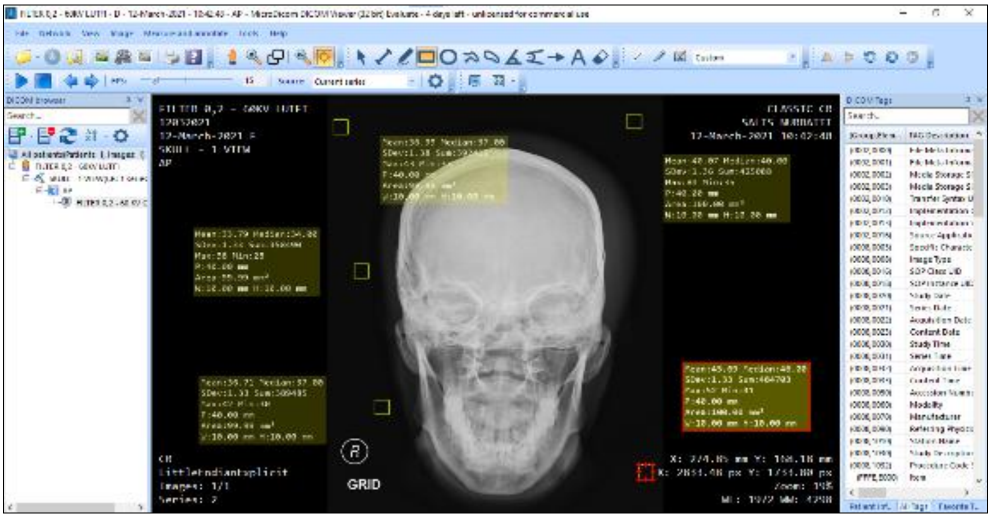

Fig 3: ROI positions at five different background locations

ROI creation is performed by pressing the "ROI" button on the Micro Dicom Viewer interface. The ROIs are drawn manually and carefully, with their sizes adjusted according to the predetermined dimensions. The mean pixel intensity within the ROI and the standard deviation of the background pixels are then displayed automatically on the right side of the screen when the ROI button is pressed. The resulting images, along with the measured mean pixel intensity within the ROIs and the background pixel standard deviation for all regions—bone tissue, soft tissue, and background—are presented in Figures 2 and 3.

After measuring the mean pixel intensity and standard deviation across all ROIs in the bone tissue, soft tissue, and background, the signal-to-noise ratio (SNR) was calculated using Equation 2.

$$SNR = \frac{I}{\delta_b} \quad (2)$$

Where I and δ_b was the signal intensity at the object ROI and the standard deviation at the background ROI. The contrast-to-noise ratio (CNR) was calculated by subtracting the mean pixel intensity of the bone tissue ROIs from the mean pixel intensity of the soft tissue ROIs and dividing by the standard deviation of the background ROIs. The CNR value was computed using Equation 3.

$$CNR = \frac{\left|ROI_{organ} - ROI_{background}\right|}{\sqrt{\frac{1}{2}\times\left({\delta_o}^2 + {\delta_b}^2\right)}} \quad (3)$$

where ROI_o and ROI_b represent the object and background region of interest, respectively. δ_o and δ_b was the standard deviation of the signal intensity at the object and background ROIs, respectively. The contrast is defined as the difference between the mean pixel intensity in the hard-tissue ROI in the forehead region and the mean pixel intensity in the soft-tissue ROI, and the standard deviation of the pixels is obtained from five background ROI locations.

Results

Effect of Exposure Factors on SNR Values in Head Phantom Radiographic Images

One image quality parameter is SNR, which describes the difference between the measured signal intensity and the noise level in an image. The higher the resulting SNR value, the easier it is to distinguish between signal and noise (Louk & Suparta, 2014) [11]. SNR is essential because it can affect the diagnostic process of a disease based on the imaging results. Table 2 presents the SNR values for the head phantom images.

Table 2: SNR of the bone tissue of the head phantom

		SNR value				
Voltage (kV)	**Current-Time (mAs)**	**No Filter Zn**	**Filter Zn 0,2 mm**	**Filter Zn 0,4 mm**	**Filter Zn 0,6 mm**	**Filter Zn 0,8 mm**
60	50	2418,66	2340,10	2339,82	2004,14	1507,39
65	40	2240,36	2257,05	2206,75	1876,99	1392,40
70	32	2188,92	2173,04	2070,81	1688,11	1342,03
75	25	2187,83	2153,73	1931,27	1011,07	1238,52
80	20	2187,68	2052,81	1782,14	1068,11	1160,25

Based on Table 2, which shows the relationship between SNR and increasing tube voltage in this study, the SNR value decreases as the tube voltage (kV) increases, in contrast to the effect of increasing tube current–time product (mAs). In Table 2, which shows SNR as a function of mAs, the higher the mAs, the higher the SNR.

Table 2 shows that the highest SNR for the head phantom image is obtained without additional filtration at 60 kV. In contrast, the lowest SNR value for the head phantom image is obtained with a 0.6 mm filter at 75 kV. From Table 2, it can be analyzed that increasing exposure time (mAs) increases SNR. For the condition with a 0.6 mm filter, 70 kV, and 32 mAs, the SNR shows a marked increase because there is a significant difference between the SNR for 0.6 mm filtration at 75 kV and 25 mAs (1011.07) and that for 0.6 mm filtration at 70 kV and 32 mAs (1688.11). However, the SNR value for 0.6 mm filtration at 80 kV and 18 mAs (1068.11) is slightly higher than that for 0.6 mm filtration at

75 kV and 25 mAs. This is due to the substantial increase in image intensity with the 0.6 mm filter thickness, leading to significant noise.

Table 3: SNR of the soft tissue of the head phantom

SNR value						
Voltage (kV)	**Current-Time (mAs)**	**No Filter Zn**	**Filter Zn 0,2 mm**	**Filter Zn 0,4 mm**	**Filter Zn 0,6 mm**	**Filter Zn 0,8 mm**
60	50	304,69	302,58	383,54	319,84	232,48
65	40	319,08	302,76	329,94	313,87	226,71
70	32	321,81	339,62	318,26	307,08	226,11
75	25	331,91	371,36	288,67	212,87	219,70
80	20	339,47	371,02	272,01	212,41	219,76

The SNR values of the soft tissue in the head phantom images were obtained by dividing each image into five measurement points. These points were located around the periphery of the image, encircling it from right to left, and the resulting values were then averaged. Table 3 presents the SNR values for the soft-tissue images of the head phantom. The SNR is influenced by the mean soft-tissue intensity, obtained by averaging measurements from five locations, and by the background noise, obtained by averaging measurements from five locations. The highest SNR in soft tissue was 383.54, obtained with a 0.4 mm filter at 60 kV and 50 mAs. SNR is a quantitative parameter of image quality; a higher SNR indicates better image quality (Song *et al*., 2004) [13].

Table 3 showed the relationship between SNR magnitude and Zn filter thickness for different tube voltages (kV) and mAs settings. The calculated soft-tissue SNR values in the head phantom are fluctuating. The 0.8 mm filter shows a relatively narrow range of SNR values, forming an almost homogeneous pattern. In contrast, for the conditions without a filter and with a 0.2 mm filter, the SNR tends to increase as the tube voltage increases and the mAs decreases. Meanwhile, for filters from 0.4 mm to 0.6 mm, the resulting SNR values tend to decrease. This occurs because the mean pixel intensity in soft tissue fluctuates, so when divided by the background standard deviation, the resulting soft-tissue SNR values become highly variable.

Effect of Exposure Factors on CNR Values in Head Phantom Radiographic Images

Table 4: CNR of the bone tissue of the head phantom

CNR value						
Voltage (kV)	**Current-Time (mAs)**	**No Filter Zn**	**Filter Zn 0,2 mm**	**Filter Zn 0,4 mm**	**Filter Zn 0,6 mm**	**Filter Zn 0,8 mm**
60	50	2113,97	2037,52	196,27	1684,29	1274,74
65	40	1921,28	1954,29	1876,80	1563,11	1163,12
70	32	1867,10	1833,41	1752,54	1381,03	1115,91
75	25	1855,92	1782,37	1642,60	798,20	1018,64
80	20	1848,20	1681,78	1510,13	855,7	940,49

The calculated CNR values for the head phantom radiographic images are presented in Table 4, which indicates the threshold at which the object becomes visible in this study: a CNR of 798.20. Furthermore, Table 4 shows that the CNR values at exposure times of 25 mAs and 20 mAs differ only slightly. This indicates that the image quality at 25 mAs and 20 mAs is not significantly different.

The relationship between CNR and tube voltage showed that a higher tube voltage (kV) was associated with lower CNR. Likewise, Table 4 shows that, for each tube voltage, the thicker the filter, the lower the CNR, resulting in curves with varying downward trends. For the 0.6 mm filter, the graph shows that at 75 kV with 25 mAs, the CNR is lowest compared with 80 kV and 20 mAs, although the difference is minimal. This is due to increased X-ray penetration through the material, leading to an uneven distribution of X-ray intensity and affecting the quality of the resulting radiographic image, even when the object is the same thickness; this phenomenon is known as the anode heel effect (Alfiati, 2013) [1].

Discussion

The X-ray tube voltage is the potential difference between the cathode and anode required to accelerate electrons from the cathode filament to the anode surface. The voltage (kV) set by the radiographer determines the speed of the electrons as they travel from the cathode to the anode. The speed of the electrons increases as the tube voltage (kV) applied to the X-ray tube increases. The faster the electrons move, the greater the X-ray energy produced. The higher the X-ray energy, the greater the penetrating power to pass through tissue. Therefore, the tube voltage (kV) affects the quality of the X-rays produced (Aryawijayanti, 2015) [2].

In a study by Labania *et al*. (2021) [9], it was reported that as tube voltage (kV) increases, SNR decreases. This study obtained similar results: as the tube voltage (kV) increases, the resulting SNR tends to decrease. This occurs because higher tube voltage (kV) reduces image intensity, so when it is divided by the noise level, the SNR is lower. At 75 kV with a 0.6 mm filter, the SNR value tends to be lower than the SNR at 80 kV with a 0.6 mm filter. This relates to one of the X-ray tube's characteristics: the anode angle. The focal target for electrons emitted from the cathode is the anode, which is located inside the X-ray tube. However, the anode angle causes an uneven distribution of X-ray intensity even when the object is uniform in thickness, which affects the resulting radiographic quality; this phenomenon is known as the anode heel effect. To achieve a uniform X-ray intensity, the positioning of the object receiving the radiation is therefore very important (Alfiati, 2013) [1].

In addition to the anode angle, image formation is also influenced by exposure factors, particularly the X-ray tube voltage (kV). The X-ray unit produces X-rays with different energies depending on the applied voltage, which in turn results in different penetration powers. The higher the tube voltage used, the greater the resulting penetration power (Litasova *et al*., 2018) [10]. This relates to the increase in X-ray intensity, which reflects the total photon energy emitted by the tube. Variations in tube voltage directly affect the resulting intensity (Fauber, 2012) [6].

An increase in SNR will improve digital image quality. A higher SNR indicates that the signal strength is greater than the noise level. Conversely, a decrease in SNR occurs when the noise increases relative to the signal strength. The higher the SNR, the better the image quality; in other words, the image with the highest SNR is considered optimal. Good image quality means the image can display anatomical structures in sufficient detail for disease diagnosis (Fauber, 2012) [6].

The CNR parameter describes how well the signal can be distinguished from the background; the higher the contrast, the easier it is to differentiate the signal from the background. Contrast is the difference in brightness between the regions that form a radiographic image. The lower the density value, the higher the resulting contrast, and since contrast is related to CNR, a higher CNR value indicates that the signal is more easily distinguished from the background. The relationship between CNR and radiographic image quality is that images with high CNR values are easier to interpret diagnostically. In contrast, images with low CNR values are more challenging to diagnose (Wibowo *et al*., 2016) [16]. The object ROI mean influences the CNR value, the background ROI mean, and the background noise.

At different current levels, as the tube current increases for each filter thickness, the CNR value also increases. The curves for the condition without a filter and for filter up to 0.4 mm show similar patterns because the CNR ranges are not very different, unlike those for the 0.6 mm and 0.8 mm filters. A previous study by Choi *et al*. (2018) [4] reported that the greater the tube current used for imaging, the higher the resulting CNR value. The same trend was observed in this study: for each Zn filter thickness, the CNR increased with increasing tube current. High CNR values make images easier to interpret diagnostically, whereas low CNR values make them more difficult to interpret (Wibowo *et al*., 2016) [16].

Conclusion

From the research, it can be concluded that as the thickness of the Zn filter increases, both the mean and background pixel intensities increase. This results in decreases in SNR and CNR with respect to tube voltage (kV), but increases in SNR and CNR with respect to tube current-time product (mAs). For the soft tissue, the highest SNR value was obtained with a 0.4 mm Zn filter, which was 383.54, while the highest SNR value for the hard tissue was found without the Zn filter, at 2418.66, and the highest CNR value was also found without the Zn filter, at 2113.97.

References

1. Alfiati. Studi Efek Heel pada Film Radiografi, 2013.
2. Aryawijayanti R. Analitisi Dampak Radiasi Sinar X pada Mencit Melalui Pemetaan Dosis Radiasi di Laboratorium Fisika Medik, 2015.
3. Bushong SC. Radiologic Science for Technologist Physics Biology and Protection, 2001.
4. Choi HR, Kim RE, Heo CW, Kim CW, Yoo MS, Lee Y. Optimization of Dose and Image Quality Using Self Produced Phantom with Various Diameters in Pediatric Abdominal CT Scan. Optik,2018:168:54–60.
5. Fahmi A, Firdausi KS, Budi WS. Pengaruh Faktor Eksposi Pada Pemerikasaan Abdomen Terhadap Kualitas Radiograf Dan Paparan Radiasi Menggunakan Computed Radiography. Berkala Fisika, 2008, 11(4).
6. Fauber TL. Radiographic Imaging and Exposure Fourth Edition, 2012.
7. Fosbinder R, Orth D. Essentials of Radiologic Science, 2002.
8. Khasanah K. Analisa Pengaruh Peningkatan Tegangan Tabung Sinar X terhadap Kualitas Citra Radiograf dan Radiasi Hambur pada Pemeriksaan Thorax, 2018.
9. Labania HM, Rindayani P, Kasman, Abd Rahman, Ulum S. Analisis Kontras Digital Radiography Dengan Menggunakan ImageJ. Gravitasi,2021:20(1):10–18.
10. Litasova S, Hidayanto E, Azam M, Fisika D, Sains F, Diponegoro U, *et al*. Pengaruh ketebalan dan kombinasi jenis filter terhadap nilai Entrance Skin Exposure ESE menggunakan faktor eksposi pemeriksaan kepala. Youngster Physics Journal, 2018, 7(2).
11. Louk AC, Suprata GB. Pengukuran Kualitas Sistem Pencitraan Radiografi Digital Sinar X. BIMIPA,2014:24(2):149–166.
12. Pardede DDM, Setiawati E. Perhitungan Nilai Dosis Dan Kontras Citra Computed Radiography CR Dengan Variasi Ketebalan Dan Kombinasi Jenis Filter. Youngster Physics Journal, 2014, 3(4).
13. Song X, Pogue BW, Jiang S, Doyley MM, Dehghani H, Tosteson TD, *et al*. Automated Region Detection Based on The Contrast to Noise Ratio in Near Infared Tomography. Applied Optics,2004:43(5):1053–1062.
14. Sparzinanda E, Nehru N, Nurhidayah N. Pengaruh Faktor Eksposi Terhadap Kualitas Citra Radiografi. Journal Online of Physics, 2018, 3(1).
15. Trirahayu I. Variasi Faktor Eksposi dan Ketebalan Filter Cu untuk Optimalisasi Citra Radiograf, 2013.
16. Wibowo NPE, Susilo, Sunarno. Uji Profisiensi Citra Hasil Eksposi Sistem Radiografi Digital di Laboratorium Fisika Medik Unnes. Unnes Physics Journal,2016:1(2):527–539.